Lithographically patterned fiber bundles for in-vivo Raman spectroscopy

J.B. Barton, G.E. Carver*, S.K. Chanda, W.J. Cote, S.A. Locknar
Omega Optical LLC, Brattleboro, VT 05301

Manish Gupta Nikira Labs Inc.
Mountain View, CA 94043

Presented at SPIE BiOS, January 2022

Proceedings Volume 11953, Optical Fibers and Sensors for Medical Diagnostics, Treatment and Environmental Applications XXII; 119530G (2022) https://doi.org/10.1117/12.2610041

Lithographically patterned fiber bundles for in-vivo Raman spectroscopy

J.B. Barton, G.E. Carver*, S.K. Chanda, W.J. Cote, S.A. Locknar
Omega Optical LLC, Brattleboro, VT 05301 USA

Manish Gupta
Nikira Labs Inc.
Mountain View, CA 94043

ABSTRACT

Raman spectroscopy can be used extensively, from handheld substance identification systems to in-vivo cancer detection. The ability to quickly and non-invasively identify compounds based on intrinsic vibrational signatures has seen Raman applications skyrocket in recent years - many using fiber optic probes. This paper describes the modeling, deposition, lithographic patterning, and testing of filters directly deposited onto the distal tip of a fiber bundle. These spectrally sharp bandpass and long pass filters allow for the detection of Raman scattering down to about 200 cm^{-1}. Blocking of laser radiation above OD6 is enabled by coating both the distal and proximal tips.

Keywords: Interference filters, optical fiber bundles, lithography, Raman spectroscopy

1. INTRODUCTION

Raman spectroscopy can be used extensively, from handheld substance identification systems to in-vivo cancer detection. The ability to quickly and non-invasively identify a variety of compounds based on intrinsic vibrational signatures has seen Raman applications skyrocket in recent years[1,2,3]. As shown in figure 1, a promising application of the technology presented below is the possibility of performing in-situ Raman spectroscopy in a biopsy needle. Many in-situ Raman methods rely on using free-space filters, and are therefore unable to block Raman scattering from the optical fiber in the zero to 1500 cm^{-1} range. As a result, researchers only look at Raman features at higher wavenumbers (e.g. 2400 – 3800 cm^{-1}) where there is negligible background from fiber scattering. This scheme has seen limited success for in vivo measurements because it misses the critical Raman fingerprint region (500 – 1500 cm^{-1}) which provides substantially more chemical information and can result in higher sensitivity and specificity. For example, in order to make accurate non-invasive blood glucose measurements using Raman spectroscopy, the analysis must include Raman scattering from 550 – 1680 cm^{-1}, a region often obscured by Raman scattering within the laser delivery fiber. By both bandpass filtering the delivered laser light and long-pass filtering the collected scattering, the patterned bundle presented below is able to detect Raman scattering down to 200 cm^{-1} and probe specific molecular features in the "fingerprint region".

Conventional Raman systems use free-space bandpass filters to remove laser side bands, spontaneous backgrounds, and inelastic scatter from the fiber itself. Light collection pathways typically use additional free-space filters to remove residual elastically scattered laser light down to about OD6. Fiber tip coating capabilities at Omega Optical [4,5,6] have been leveraged to integrate bandpass and long pass filters with Raman fiber bundles. The integration was initially done by coating individual fibers and subsequently assembling the fiber bundle. This paper describes the modeling, deposition, lithographic patterning, and testing of filters directly deposited onto the distal tip of a Raman fiber bundle. The lithographic process involves two masks for isolating the excitation and collection fibers. For maximal collection efficiency, the detection fibers in Raman probes must have large multimode cores.

* gcarver@omegafilters.com; phone 1 802 251-7346; www.omegafilters.com

This causes a distribution in the angles of incidence at the coated tip that must be considered when designing the filter. A laser pumped tunable light source is used to test the coatings. These spectrally sharp bandpass and long pass filters indeed allow for the detection of Raman scattering down to about 200 cm-1. Blocking of the laser radiation above OD6 is enabled by coating both the distal and proximal tips of the probe. The following sections describe modeling, deposition, lithographic patterning, and testing of filters directly deposited onto the distal tip of a fiber bundle.

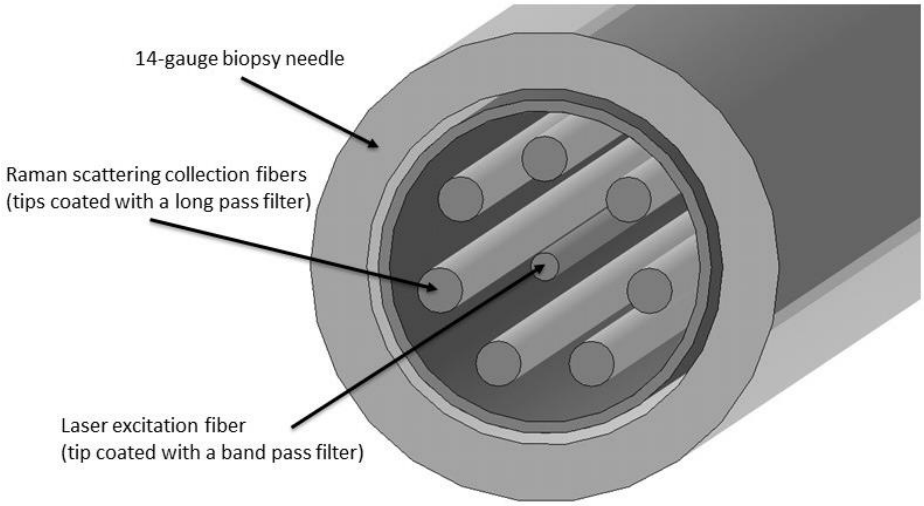

Figure 1. Schematic showing how a Raman fiber probe can be used in a biopsy needle to provide in-situ medical diagnostics

2. DESIGN, DEPOSITION, AND TESTING

The band pass (BP) and long pass (LP) designs shown in figures 2 and 3 are interference stacks composed of high index and low index layers. The fiber bundle depicted in figures 1 and 4 positions seven optical fibers around a central fiber. The central fiber transmits laser excitation through a 105 micron diameter core with a 125 micron clad. The seven surrounding fibers collect Raman scatter through 200 micron diameter cores with 220 micron clads. Both fiber types have a numerical aperture (NA) of 0.22, which means that the maximal external angle is about 12.7 degrees. Our goal is to deposit the LP on the seven outer fibers, and to deposit the BP on the central fiber. Spectrally steep filters allow for the collection of Raman spectra close to the laser wavelength at low wavenumbers. The BP is a 4-cavity Fabry-Perot design with a spectral width of 10 nm. The BP models in figure 2 show a typical spectral shape for an angle of incidence (AOI) of zero degrees, and a distorted plus blue-shifted spectral shape for an AOI of 12.5 degrees. The LP has 220 layers such that the transition from blocking to transmission occurs within a minimal number of nm – steeper than our earlier work [6]. The models in figure 3 show a sharp edge at zero degrees, and a blue-shifted edge with a step at 12.5 degrees. The step is caused by splitting between the s and p polarization states. The step can be avoided by increasing the effective index of the design – typically by replacing the high in a high/low pair with three highs. The three highs were not used in this work because the single high design allows for a steeper edge and the distribution of angles supported by the fiber's modes will wash out the step. The spectral blue shifts with increasing angle are a function of the internal angle φ which can be calculated from the effective refractive index of the film and the external angle. The passband of a filter shifts to shorter wavelengths according the value of $\cos \varphi$.

Fiber tips are coated using a plasma assisted reactive magnetron sputtering (PARMS) system. Low to moderate temperature processes are appropriate for coating optical fiber bundles. The PARMS machine deposits niobium oxide (n

at 500 nm = 2.403) and silicon oxide (n at 500 nm = 1.479). This process deposits robust hard oxides. There are eleven pockets that usually hold flat substrates. Custom jigs fit in these pockets and hold the fiber bundles during deposition.

Spectral performance of the coated fiber bundles is measured with a 1 nm spectral resolution using a tunable light source from Energetiq and a linear power meter from Newport. Deep optical density can be tested with this setup, which provides a dynamic range from milliwatts to picowatts.

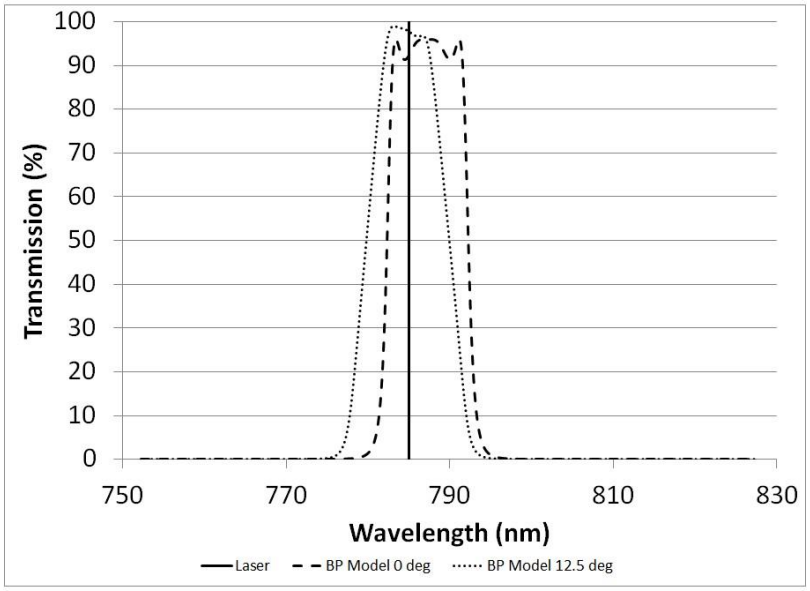

Figure 2. Models of transmission versus wavelength for a band pass filter at zero and 12.5 degrees (laser at 785 nm)

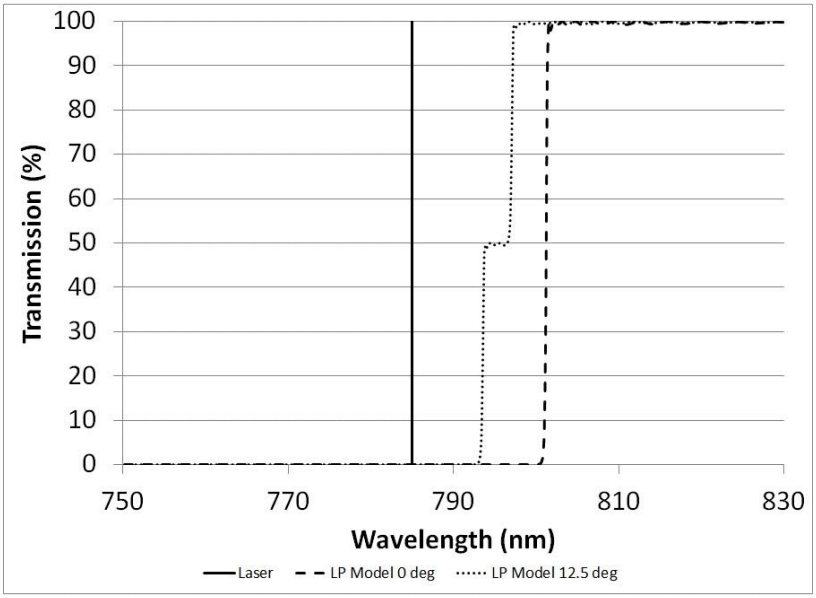

Figure 3. Models of transmission versus wavelength for a long pass filter at zero and 12.5 degrees (laser at 785 nm)

3. LITHOGRAPHIC PATTERNING

During the lithographic processing sequence, a photoresist pattern is first formed, followed by deposition of the interference stack, and then liftoff of unwanted material. Any coating that lands on the resist is removed when the resist is stripped during liftoff. As shown in figure 4, there are two masks - mask #1 blocks the central fiber, and mask #2 blocks the peripheral fibers. The process sequence is shown on figure 5. Resist is first defined by mask #1. The long pass (LP) is deposited, and after liftoff #1, the LP coating remains over the peripheral fibers but not over the central fiber. Next, resist is defined by mask #2. The band pass (BP) is deposited, and after liftoff #2, the BP coating remains over the central fiber but not over the peripheral fibers.

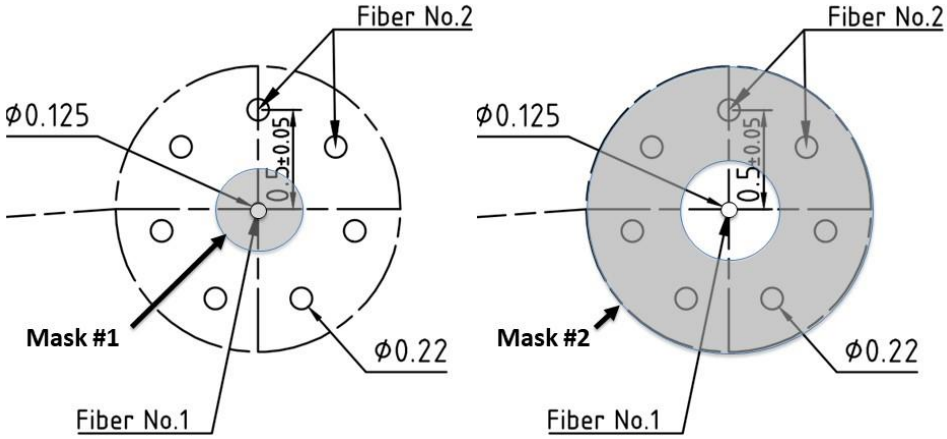

Figure 4. Bundle geometry including mask #1 and mask #2

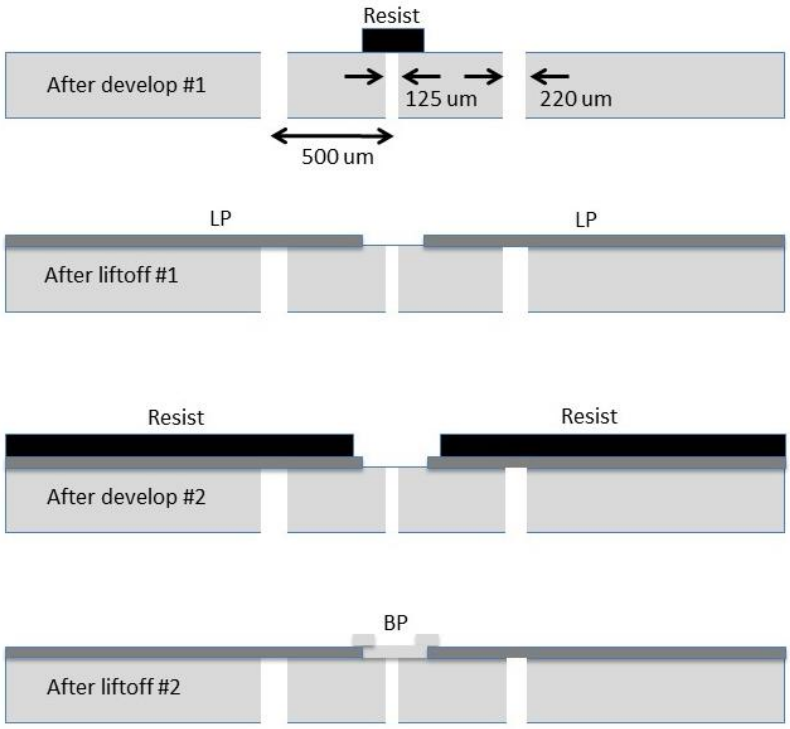

Figure 5. Lithographic process sequence

4. RESULTS

The PARMS process has been used to deposit robust coatings up to 30 microns thick on optical fiber tips. Figures 6 and 7 show transmission and optical density versus wavenumber for the BP and LP filters measured on discrete optical fibers. The curves labeled "average models" show the average over all angles supported by the fibers. Note that the average models match the data rather well – confirming that the peak wavelength blue-shifts from the zero-degree model by a few nm. Blocking at the laser wavelength reaches nearly OD6 with one coated end. The LP can be applied to both ends to reach significantly higher levels of optical density at the laser wavelength. Figure 7 shows that these spectra allow for Raman collection down to about 200 cm^{-1}. Other measurements show that the LP transmits out to 1.1 microns - allowing for the collection of Raman spectra from 200 to 3800 cm^{-1}.

Figure 8 shows resist patterns after development using mask #1 and mask #2. The pitted metallic surface between the fibers was observed as-received from the supplier, and was unchanged during the lithographic and deposition processes. The fully processed fiber bundle was also measured with the above test set. Spectral curves measured on the bundle exhibited steep features similar to those in figures 6 and 7. The LP edge was, however, somewhat displaced to longer wavelengths - allowing the observation of Raman scatter down to 370 cm^{-1}. This shift can easily be adjusted in subsequent work. Figure 9 shows Raman scatter from naphthalene acquired with both the coated fiber bundle and a commercial fiber probe. In both cases, the naphthalene spectra were flattened by subtracting spectra taken on a graphite sample. This comparison is relevant because the bulky commercial probe uses optical fiber for both excitation and collection coupled with free space filters. As implied in figure 7, the BP filter on the bundle prevents scatter within the excitation fiber from reaching the collection fibers. It should be noted that pinholes and/or defects in the LP filter limited optical density at 785 nm. This was remedied for the measurement shown in figure 9 by adding an additional OD4 LP filter near the detector within the Raman test set. This can also be done by adding the LP to the proximal end of the bundle.

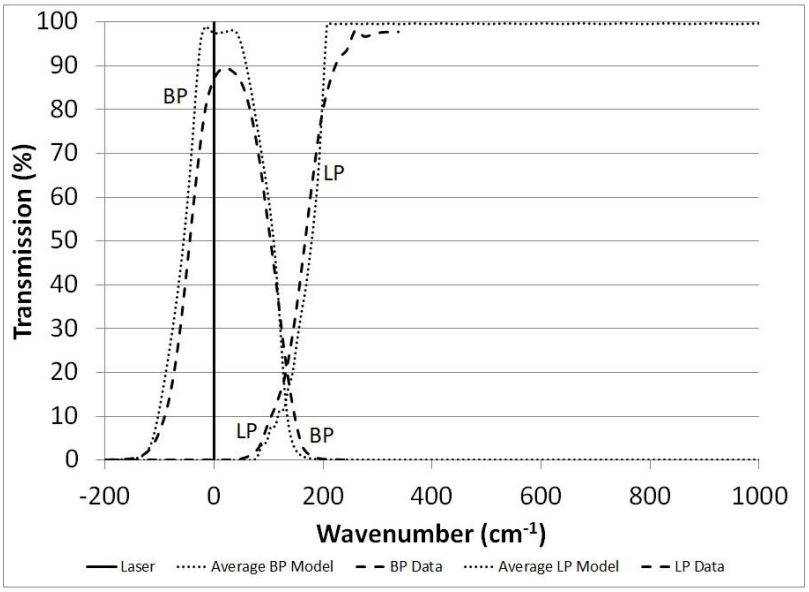

Figure 6. Transmission versus wavenumber for BP and LP filters

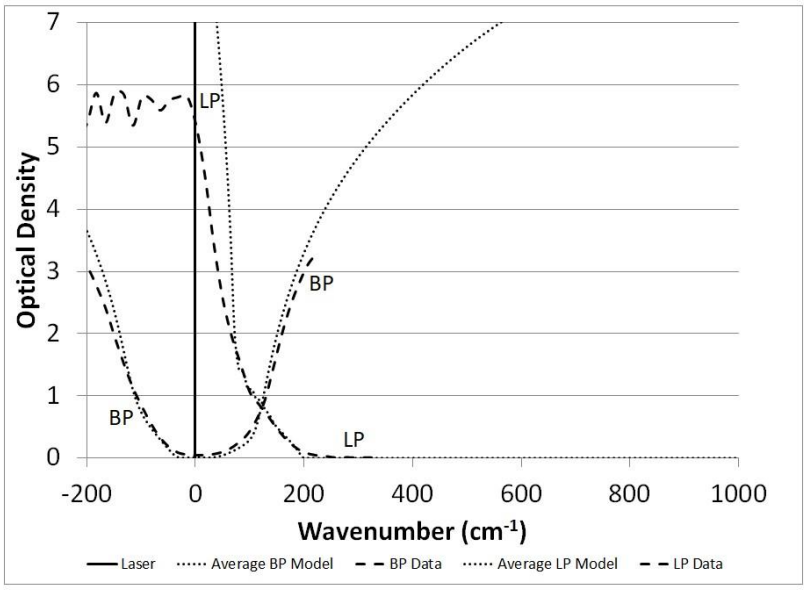

Figure 7. Optical density versus wavenumber for BP and LP filters

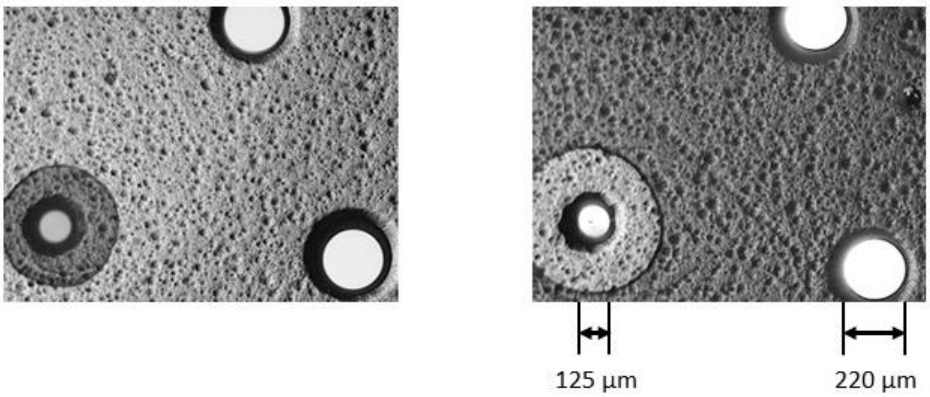

Figure 8. Images of bundle's central region after development using mask #1 (left) and after mask #2 (right)

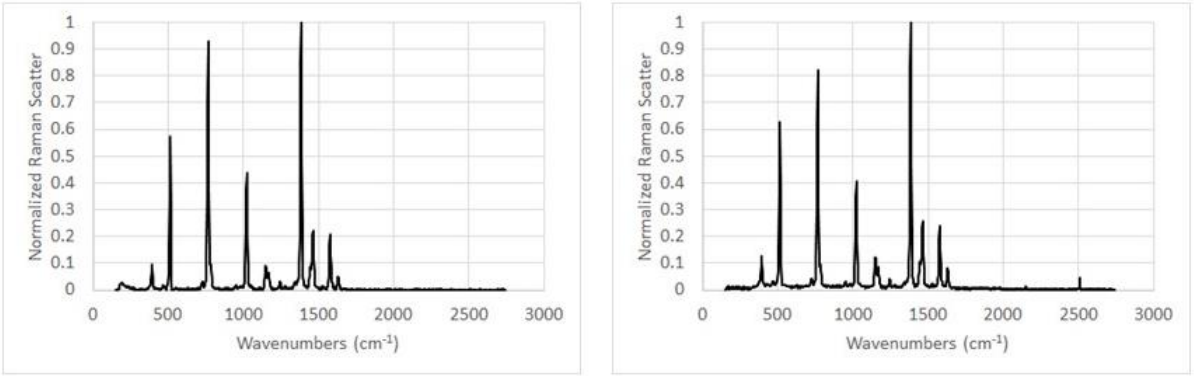

Figure 9. Raman spectra of naphthalene using a commercial fiber-coupled probe (left), and the patterned fiber bundle (right)

5. CONCLUSIONS

Omega deposits complex dielectric stacks on fiber tips for a multitude of applications. Endoscopic Raman spectroscopy is a growing example [7]. The lithographically patterned coatings described in this paper allow for Raman scatter to be observed from 200 to 3800 cm^{-1}. The low wavenumber limit is a function of both spectral steepness of the coatings and the modes supported by the fibers. Ongoing efforts will optimize tip geometry to maximize light collection for biomedical applications. Translational activities for future applications will include new bundle configurations and high yield production.

REFERENCES

[1] L.F. Santos, R. Wolthuis, S. Koljenović, R.M. Almeida, G.J. Puppels, "Fiber-optic probes for in vivo Raman spectroscopy in the high-wavenumber region", Analytical chemistry, 77(20), pp.6747-6752 (2005); https://doi.org/10.1021/ac0505730

[2] I.Gusachenko, M. Chen, K. Dholakia, "Raman imaging through a single multimode fibre", Optics Express, 25(12), pp.13782-13798 (2017); https://doi.org/10.1364/OE.25.013782

[3] N. Li, H. Zang, H. Sun, X. Jiao, K. Wang, T.C.Y. Liu, Y. Meng, "A Noninvasive Accurate Measurement of Blood Glucose Levels with Raman Spectroscopy of Blood in Microvessels". Molecules, 24(8), p.1500 (2019); doi: 10.3390/molecules24081500

[4] J.B. Barton, S.K. Chanda, S.A. Locknar, G.E. Carver "Interference filters deposited on optical fiber tips", Proc. SPIE 11889, Optifab 2021, 1188901 (28 October 2021); https://doi.org/10.1117/12.2601854

[5] J.B. Barton, S.K. Chanda, S.A. Locknar, G.E. Carver, "Coated fiber tips for optical instrumentation," Proc. SPIE 9754, (2016); DOI: 10.1117/12.2211083

[6] J.B. Barton, G.E. Carver, S.K. Chanda, S.A. Locknar, M. Gupta "Fiber bundles with integrated bandpass and notch filters for in-vivo Raman spectroscopy", Proc. SPIE 11233, Optical Fibers and Sensors for Medical Diagnostics and Treatment Applications XX, 112330S (20 February 2020); https://doi.org/10.1117/12.2546207

[7] M. T. Gebrekidan, A. S. Braeuer, "Filter-coated Raman fiber bundle probe and deep neural networks for oral cancer diagnostics," in OSA Optical Sensors and Sensing Congress 2021 (AIS, FTS, HISE, SENSORS, ES), OSA Technical Digest (Optical Society of America, 2021); https://doi.org/10.1364/SENSORS.2021.STu4H.5